Supporting Information

A Computational Experiment to Study Hydrogenations of Various Unsaturated Compounds Catalyzed by a Rationally Designed Metal-free Catalyst

*Lili Zhao, Gang Lu, Fang Huang, and Zhi-Xiang Wang**

SI1. Energetic and geometric results for the borohydride elimination in **1** to give (2,6-Me-Ph)$_2$B-H and 1,2,3,4-tetrahydro pyridine

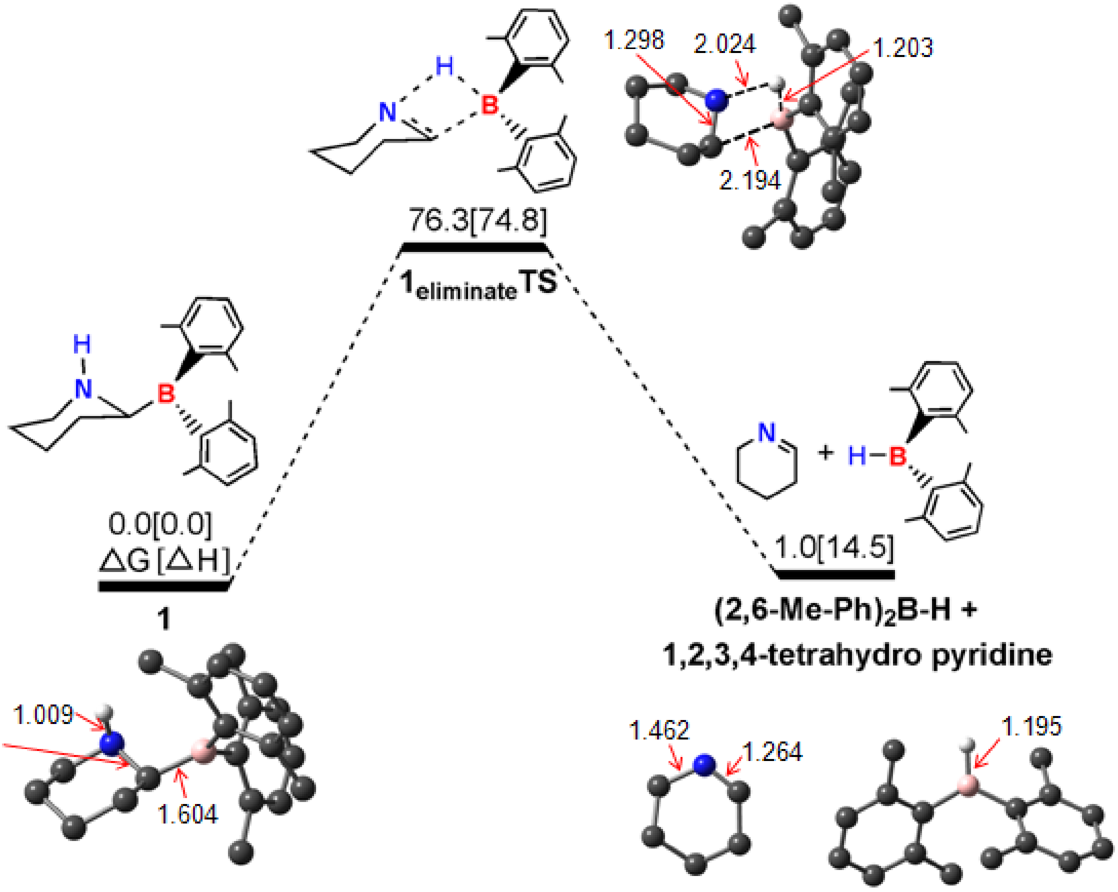

Fig. S1 Energetic and geometric results for the borohydride elimination in **1** to give (2,6-Me-Ph)$_2$B-H and 1,2,3,4-tetrahydro pyridine

SI2. Geometric results corresponding to Table 1

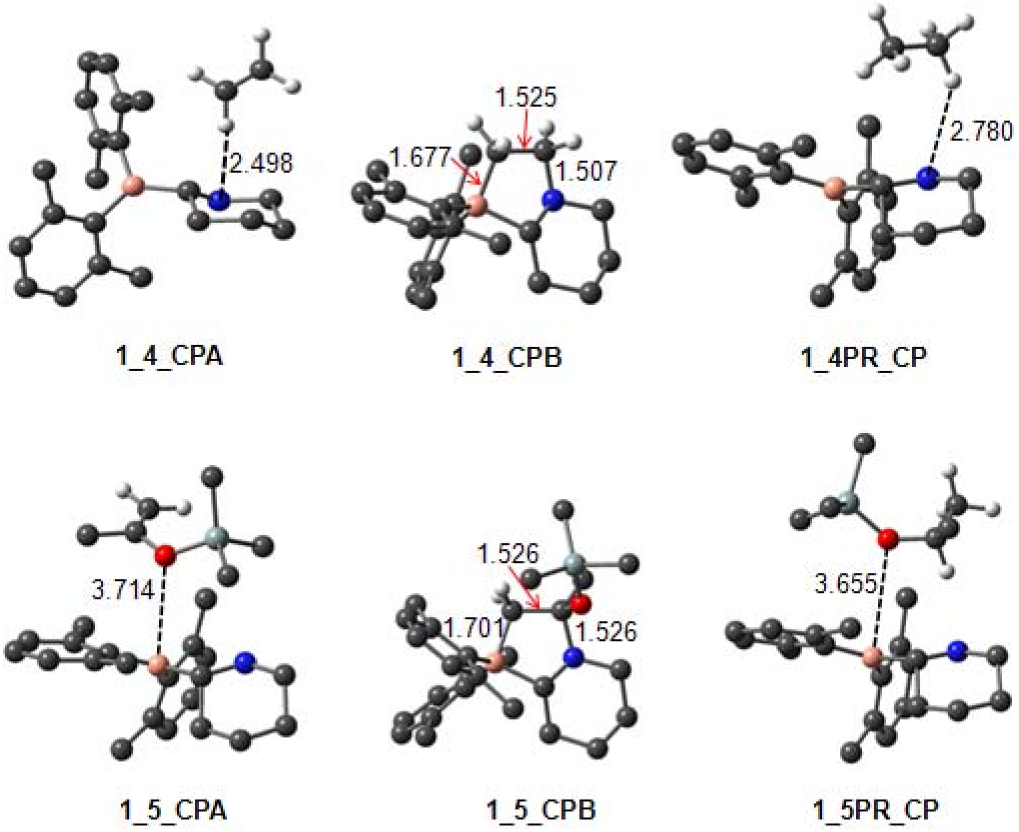

1_4_CPA 1_4_CPB 1_4PR_CP

1_5_CPA 1_5_CPB 1_5PR_CP

Fig. S2-1 M05-2X/6-311++G** optimized structures of various complexes between the catalyst (**1**), and $CH_2{=}CH_2$ (**4**) and $CH_2{=}C(Me)OSiMe_3$ (**5**). The selected atomic distances are given in Å. Trivial hydrogen atoms were omitted for clarity

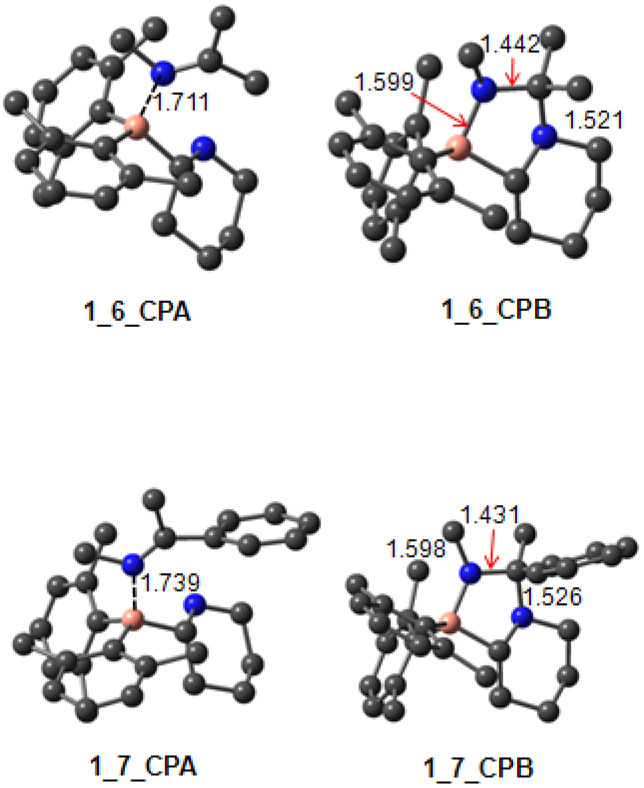

Fig. S2-2 M05-2X/6-311++G** optimized structures of various complexes between the catalyst (**1**), and imines ($Me_2C{=}NMe$ (**6**) and $Ph(Me)C{=}NMe$ (**7**)). The selected atomic distances are given in Å. Trivial hydrogen atoms were omitted for clarity

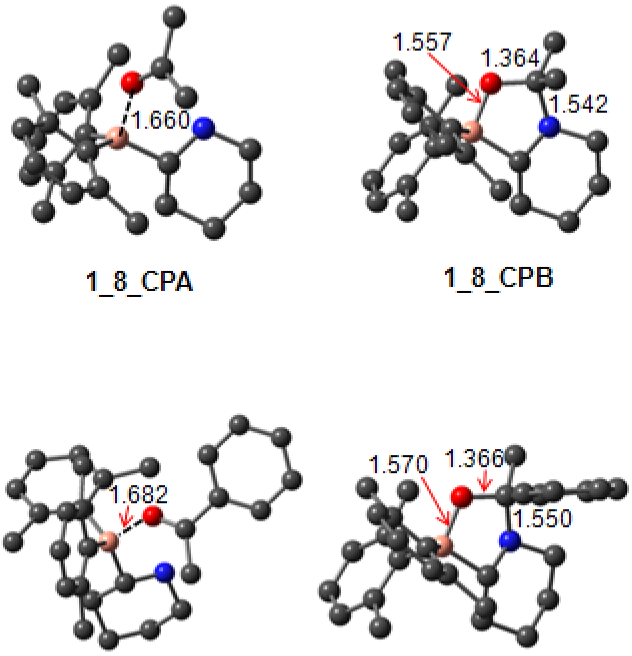

1_8_CPA 1_8_CPB 1_8PR_CP

1_9_CPA 1_9_CPB 1_9PR_CP

Fig. S2-3 M05-2X/6-311++G** optimized structures of various complexes between the catalyst (**1**), and imines ($Me_2C=O$ (**8**) and Ph(Me)C=O (**9**)). The selected atomic distances are given in Å. Trivial hydrogen atoms were omitted for clarity.

SI3. Optimized structures of CO_2 activation products mediated the experimentally prepared B/P FLP, Al/P FLP and our designed B/N FLP (**1**)

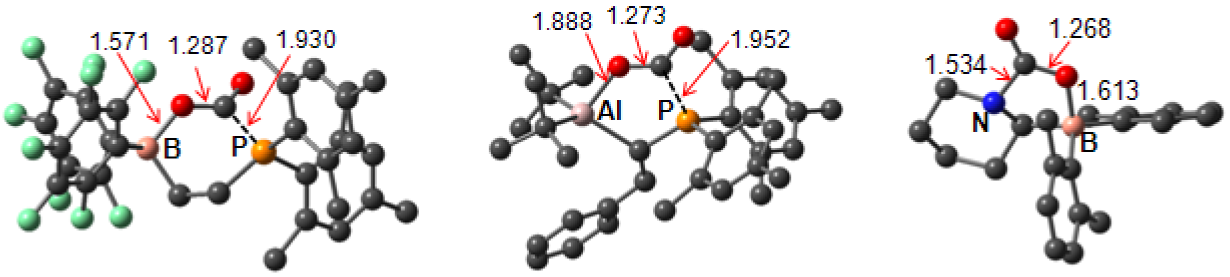

B/P_CO_2_CP Al/P_CO_2_CP 1_CO_2_CP

Fig. S3 Optimized structures of CO_2 activation products mediated by the experimentally prepared B/P FLP, B/Al FLP and our designed B/N FLP (**1**)**,** the optimized bond parameters are given in Å.

SI4. The Energetic results (in kcal mol^{-1}) for the hydrogenations of **4~9** in the gas phase

Table S4 Energetic results (in kcal mol^{-1}) for the hydrogenations of **4~9** in the gas phase.[a]

	1_H_2+X	**X_IN1**	**X_TS**	**X_IN2**	**1 + XPR**
	$\Delta G[\Delta H]$	$\Delta G[\Delta H]$	$\Delta G^{\neq}[\Delta H^{\neq}]$	$\Delta G[\Delta H]$	$\Delta G[\Delta H]$
CH_2CH_2(**4**)	0.0[0.0]	5.8[-3.7]	29.5[15.5]	-27.8[-35.8]	-35.6[-33.2]
$CH_2=C(Me)OSiMe_3$(**5**)	0.0[0.0]	2.7[-0.1]	29.4[14.2]	-20.0[-31.4]	-26.7[-25.2]
$Me_2C=NMe$ (**6**)	0.0[0.0]	-5.0[-17.7]	17.0[1.3]	-17.0[-27.0]	-21.6[-20.1]
Ph(Me)C=NMe (**7R**)[b]	0.0[0.0]	0.6[-12.8]	20.4[2.2]	-17.1[-29.8]	-21.0[-20.4]
Ph(Me)C=NMe (**7S**)	0.0[0.0]	-2.9[-14.1]	19.2[1.7]	-15.3[-27.2]	-21.0[-20.4]
$Me_2C=O$ (**8**)	0.0[0.0]	-1.4[-15.2]	12.2[-4.1]	-14.7[-26.2]	-16.1[-14.7]
Ph(Me)C=O (**9R**)[b]	0.0[0.0]	-3.2[-16.5]	11.2[-6.0]	-16.8[-28.5]	-14.0[-11.9]
Ph(Me)C=O (**9S**)	0.0[0.0]	-1.4[-14.5]	10.8[-5.1]	-17.1[-26.4]	-14.0[-11.9]

[a] At the M05-2X/6-311++G** level in the gas phase. [b] For imine Ph(Me)C=NMe (**7**) and ketone (Ph(Me)C=O (**9**), two hydrogenation pathways leading to R- and S-enantiomers, respectively, have been considered.

SI5. Chemical drawing of the structures of *t*Bu$_3$P-CH$_2$CH$_2$-B(C$_6$F$_5$)$_3$ and **1_4_CPB**

tBu$_3$P-CH$_2$CH$_2$-B(C$_6$F$_5$)$_3$ **1_4_CPB**

Fig. S5 Chemical drawing of the structures of *t*Bu$_3$P-CH$_2$CH$_2$-B(C$_6$F$_5$)$_3$ and **1_4_CPB**

SI6. Optimized structures and NBO analysis of CH$_2$=CH$_2$ (**4**) and (CH$_2$=C(Me)OSiMe$_3$ (**5**)

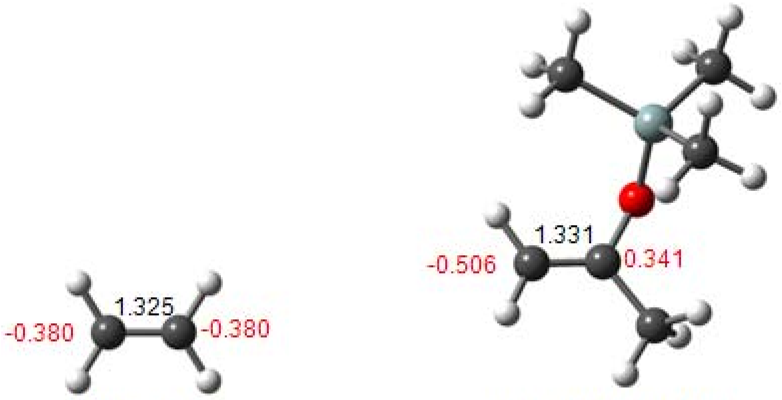

CH$_2$=CH$_2$ **CH$_2$=C(Me)OSiMe$_3$**

Fig. S6 The optimized structure of **4** and **5**. The Bond distances are colored in black and given in Å. Net charges (Q) were obtained from NBO analysis and colored in red.

SI7. The IRC results of **4_TS**

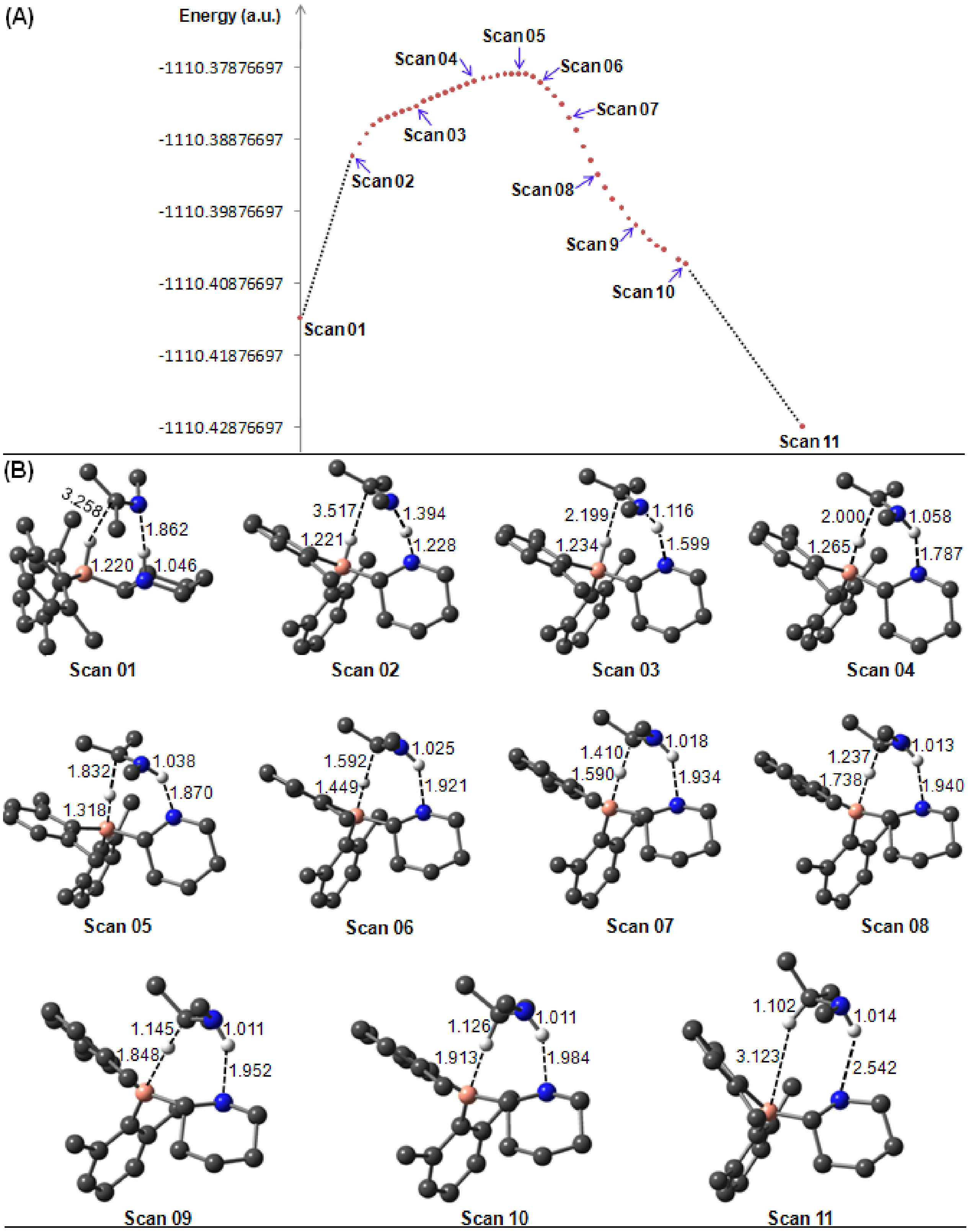

Fig. S7 (A) The IRC analysis of the transition state **4_TS** at the M052X-6-31G** level. (B) The optimized geometries (bond length in Å) on the potential energy surface (PES).

SI8. Total energies and Cartesian coordinates of all the structures

Table SI8-1. Absolute enthalpies (**H**) and Gibbs free energies (**G**) (in Hartrees) of the optimized structures of the reactions in the solvent

	H	**G**		**H**	**G**
1	-896.335302	-896.411232	**7R_IN1**	-1301.679908	-1301.779448
H_2	-1.152211	-1.166998	**7R_TS**	-1301.659395	-1301.751284
1_TS	-897.470371	-897.541605	**7R_IN2**	-1301.699708	-1301.800516
1_H_2	-897.502269	-897.575776	**7R_PR**	-405.356692	-405.402771
4_IN1	-1109.981419	-1110.072559	**7S_IN1**	-1301.681385	-1301.784393
4_TS	-1109.953548	-1110.039764	**7S_TS**	-1301.657446	-1301.750622
4_IN2	-1109.984841	-1110.080225	**7S_IN2**	-1301.695192	-1301.797122
4PR	-213.646865	-213.684572	**7S_PR**	-405.356692	-405.402771
5_IN1	-1499.176392	-1499.280775	**9R_IN1**	-1282.313002	-1282.406799
5_TS	-1499.143183	-1499.243896	**9R_TS**	-1282.298458	-1282.386101
5_IN2	-1499.202685	-1499.31017	**9R_IN2**	-1282.325686	-1282.421991
5PR	-602.866811	-602.91807	**9R_PR**	-385.971746	-386.014019
6_IN1	-1109.981419	-1110.072559	**9S_IN1**	-1282.307525	-1282.401637
6_TS	-1109.953548	-1110.039764	**9S_TS**	-1282.296648	-1282.386163
6_IN2	-1109.984841	-1110.080225	**9S_IN2**	-1282.319555	-1282.419616
6PR	-213.646865	-213.684572	**9S_PR**	-385.971746	-386.014019
8_IN1	-1090.599763	-1090.68521	**8_IN2**	-1090.61248	-1090.701594
8_TS	-1090.585925	-1090.667441	**8PR**	-194.263987	-194.297658

Table SI8-2. Absolute enthalpies (**H**) and Gibbs free energies (**G**) (in Hartrees) of the optimized structures of the reactions in the gas phase

	H	**G**		**H**	**G**
1	-896.3575658	-896.4334958	**7R_IN1**	-1301.711232	-1301.810772
H_2	-1.15548384	-1.17027084	**7R_TS**	-1301.687256	-1301.779145
1_TS	-897.4893229	-897.5605569	**7R_IN2**	-1301.73821	-1301.839018
1_H_2	-897.5159501	-897.5894571	**7R_PR**	-405.3656732	-405.4117522
4_IN1	-976.0566719	-976.1412759	**7S_IN1**	-1301.713292	-1301.8163
4_TS	-976.026135	-976.103434	**7S_TS**	-1301.687983	-1301.781159
4_IN2	-976.1078991	-976.1947201	**7S_IN2**	-1301.734166	-1301.836096
4PR	-79.74612432	-79.77366232	**7S_PR**	-405.3656732	-405.4117522
5_IN1	-1499.21644	-1499.320823	**9R_IN1**	-1282.340017	-1282.433814
5_TS	-1499.177652	-1499.323776	**9R_TS**	-1282.323225	-1282.410868
5_IN2	-1499.250408	-1499.357893	**9R_IN2**	-1282.359181	-1282.455486
5PR	-602.8829657	-602.9342247	**9R_PR**	-385.9751975	-386.0174705
6_IN1	-1110.0074	-1110.09854	**9S_IN1**	-1282.336791	-1282.430903
6_TS	-1109.977229	-1110.063445	**9S_TS**	-1282.321852	-1282.411367
6_IN2	-1110.022219	-1110.117603	**9S_IN2**	-1282.355772	-1282.455833
6PR	-213.653797	-213.691504	**9S_PR**	-385.9751975	-386.0174705
8_IN1	-1090.624991	-1090.710438	**8_IN2**	-1090.64255	-1090.731664
8_TS	-1090.607307	-1090.688823	**8PR**	-194.2666026	-194.3002736